Interplay of Unsaturated Phospholipids and Cholesterol in Membranes: Effect of the Double-Bond Position

Hector Martinez-Seara,* Tomasz Róg,[†‡] Marta Pasenkiewicz-Gierula,[‡] Ilpo Vattulainen,[§¶‖] Mikko Karttunen,** and Ramon Reigada*

*Department of Physical Chemistry, Barcelona University, Barcelona, Spain; [†]Biophysics and Statistical Mechanics Group, Laboratory of Physics, Helsinki University of Technology, Helsinki, Finland; [‡]Department of Biophysics, Faculty of Biotechnology, Jagiellonian University, Kraków, Poland; [§]Laboratory of Physics and Helsinki Institute of Physics, Helsinki University of Technology, Helsinki, Finland; [¶]MEMPHYS-Center for Biomembrane Physics, University of Southern Denmark, Odense, Denmark; [‖]Department of Physics, Tampere University of Technology, Tampere, Finland; and **Department of Applied Mathematics, University of Western Ontario, London, Canada

ABSTRACT The structural and dynamical properties of lipid membranes rich in phospholipids and cholesterol are known to be strongly affected by the unsaturation of lipid acyl chains. We show that not only unsaturation but also the position of a double bond has a pronounced effect on membrane properties. We consider how cholesterol interacts with phosphatidylcholines comprising two 18-carbon long monounsaturated acyl chains, where the position of the double bond is varied systematically along the acyl chains. Atomistic molecular dynamics simulations indicate that when the double bond is not in contact with the cholesterol ring, and especially with the C18 group on its rough β-side, the membrane properties are closest to those of the saturated bilayer. However, any interaction between the double bond and the ring promotes membrane disorder and fluidity. Maximal disorder is found when the double bond is located in the middle of a lipid acyl chain, the case most commonly found in monounsaturated acyl chains of phospholipids. The results suggest a cholesterol-mediated lipid selection mechanism in eukaryotic cell membranes. With saturated lipids, cholesterol promotes the formation of highly ordered raft-like membrane domains, whereas domains rich in unsaturated lipids with a double bond in the middle remain highly fluid despite the presence of cholesterol.

INTRODUCTION

Cholesterol is one of the most studied individual lipid species found in cell membranes. Nonetheless, many of its fundamental properties remain elusive, and thus the research dealing with cholesterol has increased its pace even further as it has been realized that a large variety of cellular functions are related to cholesterol. In particular, in mammalian cellular membranes (there is no cholesterol in prokaryotes or plant cells), cholesterol is one of the most important lipids and has many tasks, ranging from providing structural stability for membranes to facilitating membrane protein functions and acting as a precursor for hormones and vitamins (see Mouritsen (1) and Ikonen (2) for detailed discussions).

However, there is reason to stress that cholesterol is only just one of the many lipid species found in membranes. Let us focus here on its interactions with phospholipids with varying degrees of unsaturation due to their abundance in cell membranes. Saturated lipid acyl chains are known to interact very favorably with cholesterol, and this interplay gives rise to the formation of lipid rafts. Lipid rafts are highly ordered membrane domains that are rich in saturated lipids and cholesterol (3–6), and they have been shown to have a major role, e.g., in protein sorting and cellular signaling (7,8). Recent studies have further shown that cholesterol plays an exceptional role in rafts because it cannot be replaced by other sterols, not even by its immediate precursors (9). The relevance of unsaturated phospholipids in turn is highlighted, e.g., by membrane proteins, such as cytochrome *c*, that favor specific interactions with polyunsaturated lipids (10,11). Considering the breadth of phospholipids with varying degrees of unsaturation and the prominent importance of cholesterol, it is obviously of great importance to decipher the specific mechanisms of how cholesterol interacts with various lipids, including both saturated and unsaturated ones. Indeed, the interactions of cholesterol with unsaturated lipids have been the subject of intense studies over the past few years (12–15).

Here we address the molecular-scale interactions of cholesterol with unsaturated phospholipids, paying particular attention to understanding how the interplay of cholesterol and unsaturated lipids participates in determining the properties of related membranes. The relevance of elucidating this issue stems from the fact that the preferential position of the double bond in monounsaturated phospholipids in eukaryotic membranes is known to reside in the middle of an acyl chain (see Olsson and Salem (16) and references therein), but the reason for that selection is not understood. Obviously, this issue is broad because the lipid composition in cells is profoundly complex, which suggests that considering this issue in membranes with a realistic lipid composition is not feasible. In our previous study (17), we approached this issue by focusing on single-component lipid bilayers composed of lipids with monounsaturated acyl chains, and systematically studied the effect of shifting the double-bond position along the chain. Those studies showed that ordering within a membrane was weakest when the double bond was located in the middle of an

Submitted May 21, 2008, and accepted for publication June 19, 2008.

Address reprint requests to Ramon Reigada, Dept. of Physical Chemistry, University of Barcelona, c/ Marti i Franques 1, Pta 4, Barcelona 08028, Spain. Tel.: 34-93-4039290 E-mail: reigada@ub.edu.

Editor: Peter C. Jordan.

© 2008 by the Biophysical Society

0006-3495/08/10/3295/11 $2.00

doi: 10.1529/biophysj.108.138123

acyl chain. For comparison, other experiments have shown (18) that the main transition temperature of single-component lipid bilayers with monounsaturated acyl chains has a minimum when the double bond resides in the middle of the hydrocarbon chain, indicating that membrane order is minimized under those conditions. Both simulations and experiments therefore support the view that by favoring monounsaturated acyl chains with a double bond in the middle of a chain, nature promotes membrane fluidity.

In this article we complement our previous study (17) by including cholesterol to determine its interactions with monounsaturated lipid acyl chains, where the double-bond position is systematically translated along the chain. Through atomistic simulations, we find that the presence of cholesterol considerably amplifies the double-bond-induced effects on membrane properties. Even more importantly, we again find that membrane disorder and hence membrane fluidity are maximized when the double bond is positioned in the middle of an acyl chain. Intriguingly, the results suggest a cholesterol-mediated lipid selection mechanism in eukaryotic cell membranes. Saturated lipids interact strongly with cholesterol, resulting in the formation of raft-like membrane domains. However, since cholesterol inevitably also interacts with unsaturated lipids in domains where saturated lipids are not abundant, the choice by nature to prefer phospholipids with a double bond in the middle of an acyl chain implies that these domains remain highly fluid despite the presence of cholesterol.

The results allow a better understanding of the differential interaction between cholesterol and various phospholipid species, which may be relevant for fluid membrane domains (rich in unsaturated lipids) as well as raft formation phenomena involving saturated hydrocarbon lipid chains.

MATERIALS AND METHODS

We carried out atomic-scale molecular dynamics (MD) simulations for eight different membrane systems. All of the lipid bilayers were composed of a total of 128 phosphatidylcholine (PC) molecules with chains of length 18 carbons together with 32 additional cholesterol molecules, and 3900 water molecules. The cholesterol molar concentration was therefore 20%. One of the bilayers consisted of PC molecules with two fully saturated 18:0 stearyl chains. In the other seven systems, the chains were of the same length but both the *sn*-1 and *sn*-2 chain were *cis* monounsaturated. The position of the double bond was varied systematically and symmetrically as follows: for the *sn*-1 acyl chain between atoms $C3_3$-$C3_4$ (18:1c3), $C3_5$-$C3_6$ (18:1c5), $C3_7$-$C3_8$ (18:1c7), $C3_9$-$C3_{10}$ (18:1c9, DOPC), $C3_{11}$-$C3_{12}$ (18:1c11, divacenylphosphatidylcholine (DVPC)), $C3_{13}$-$C3_{14}$ (18:1c13), and $C3_{15}$-$C3_{16}$ (18:1c15); and for the *sn*-2 chain between atoms $C2_3$-$C2_4$ (18:1c3), $C2_5$-$C2_6$ (18:1c5), $C2_7$-$C2_8$ (18:1c7), $C2_9$-$C2_{10}$ (18:1c9, DOPC), $C2_{11}$-$C2_{12}$ (18:1c11, DVPC), $C2_{13}$-$C2_{14}$ (18:1c13), and $C2_{15}$-$C2_{16}$ (18:1c15) (Fig. 1 *a*). In the rest of this article, we refer to these bilayers by the index corresponding to the position of the double bond (the first carbon atom index in Fig. 1 *a*), and we assign the index 17 for the fully saturated distearoylphosphatidylcholine bilayer (DSPC with two 18:0 stearyl chains). Fig. 1 *a* shows the structure and the numbering of atoms in the DSPC molecule, as well as the positions of the double bonds in the unsaturated species. The numbering of atoms in the cholesterol molecule is displayed in Fig. 1 *b*.

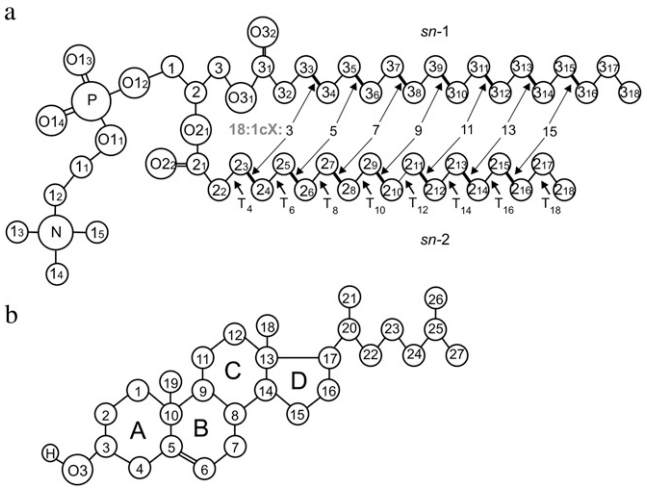

FIGURE 1 (*a*) Molecular structures of DSPC molecules with numbering of atoms and torsion angles (T). The unsaturated bonds in the other studied species are marked and numbered in the *sn*-1 chain. (*b*) Numbering of atoms for cholesterol. In both panels, the chemical symbol for carbon atoms, C, is omitted.

The initial configurations of our systems were taken from a previously equilibrated lipid bilayer with 128 dioleoylphosphatidylcholine (DOPC) and 32 cholesterol molecules homogeneously inserted into the bilayer (19). The eight different membrane systems were constructed by changing the position of the double bond as needed (for the detailed procedure, see Martinez-Seara et al. (17)).

The simulations were performed using the GROMACS software package (20,21). We used the standard united-atom force-field parameters that have been extensively tested and verified for saturated dipalmitoylphosphatidylcholine (DPPC) molecules (see, e.g., Berger et al. (22) and Patra et al. (23), and references therein). The partial charges were taken from the underlying model description (24). For the double bond, we used the description by Bachar et al. (25). The simple point charge (SPC) model (26) was used for water. For cholesterol, we used the description of Holtje et al. (27) as described in Róg et al. (28). The SETTLE algorithm (29) was used to preserve the bond lengths in water molecules, whereas the lipid bond lengths were constrained with the LINCS algorithm (30). A single 1.0-nm cutoff distance was used for the Lennard-Jones interactions (23). The long-range electrostatic interactions were handled using the particle-mesh Ewald method (31) with a real space cutoff of 1.0 nm, β spline interpolation (of order 6), and direct sum tolerance of 10^{-5}. Periodic boundary conditions with the usual minimum image convention were used in all three directions, and the time step was set to 2 fs.

The simulations were carried out in the NpT (constant particle number, pressure, and temperature) ensemble at $p = 1$ atm and $T = 338$ K. The selected temperature is above the main phase transition temperature of DSPC (T_m = 328 K)—the highest among the studied lipid species (32). The temperature and pressure were controlled by using the weak coupling method (33) with the relaxation times set to 0.6 and 1.0 ps, respectively. The temperatures of the solute and solvent were controlled independently, and the pressure coupling was applied separately in the bilayer plane (*xy*) and the perpendicular direction (*z*). The simulation protocol applied here has been successfully applied in previous MD simulations (6,17,34–37). Each simulation was run for 150 ns.

RESULTS AND DISCUSSION

Equilibration was monitored by following the time development of the area per lipid, potential energy, and tempera-

ture. It was determined that after 20 ns all of the systems had reached equilibrium (data not shown). The remaining 130 ns were used in the analysis. Here, we focus our analysis on the structural properties and calculate them separately for the different lipid double-bond positions and compare the results with those obtained without cholesterol (17). The error bars were estimated using the block analysis method (38).

Area per molecule and condensing effect

The area per lipid molecule is a basic variable that characterizes the bilayer structure. Although the area per lipid is trivial to compute in a single-component system, its definition is considerably more complicated in multicomponent systems (37,39–41). This stems from the fact that in multicomponent membrane systems it is not obvious how the cross-sectional area of a lipid should be defined and how the free area in the membrane plane should be distributed between the different molecule types. For the same reason, the volume per molecule is not well defined in many-component systems because there is no unique way to decompose the free volume to contributions occupied by individual molecule types. For further discussion of this matter, see Falck et al. (37), Edholm and Nagle (39), and Hofsäß et al. (40). We calculate the average area per PC molecule, A_{PC}, in a single-component system by dividing the total average area of the membrane, A, by the number of PC molecules in a single leaflet. For the mixed membranes, we complement this by following the procedure of Hofsäß et al. (40) that defines the area per PC as

$$A_{PC} = \frac{2A}{N_{PC}}\left(1 - \frac{N_{chol}V_{chol}}{V - N_wV_w}\right),$$

where V is the volume of the simulation box, N_{PC} is the number of PC molecules, N_w is the number of water molecules, V_w corresponds to the volume occupied by a water molecule, N_{chol} stands for the number of cholesterols, and V_{chol} is the volume of a cholesterol molecule. Essentially, this equation just expresses the point that the cross-sectional area of a lipid divided by its volume equals the area of a membrane leaflet divided by its volume. Then, A_{PC} can be computed provided that V_w and V_{chol} are known. V_w is obtained from an independent simulation of a slab of 7161 water molecules in the same simulation conditions, and cholesterol volume is taken to be 0.541 nm^3 (39).

The average areas per PC are plotted in Fig. 2 *a* as a function of the double-bond position. The numerical values are listed in Table 1. Let us first discuss the results for single-component lipid bilayers. When the double bond is moved from position 9 (corresponding to DOPC) toward the end of the chain, the limiting case being a saturated lipid (17), we find a significant reduction in the average area per PC, ~0.062 nm^2. When the double-bond position is moved from the middle of the chain toward the lipid head group, the average area per PC is reduced as well, but now the reduction is

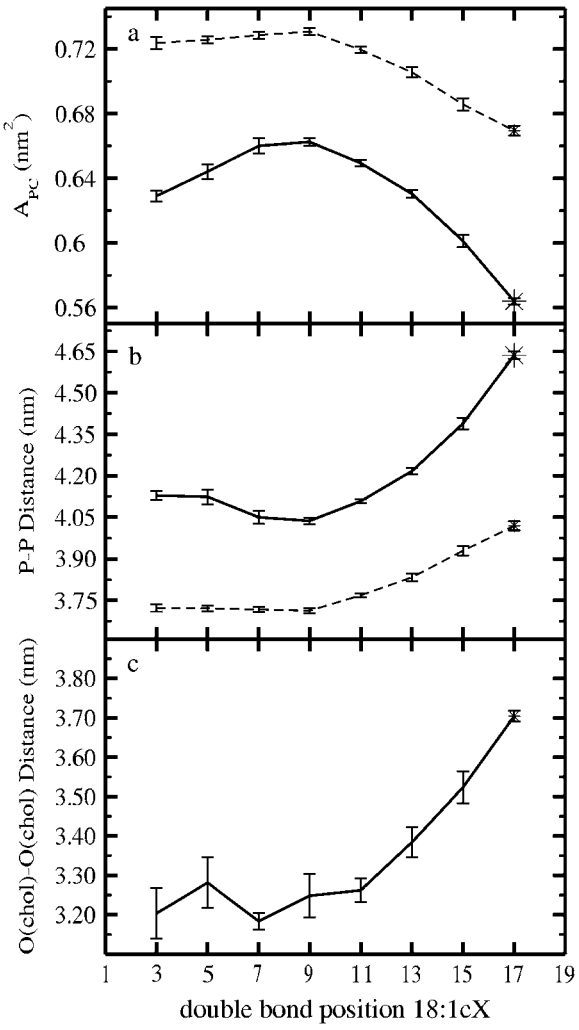

FIGURE 2 (*a*) Average surface area per PC. (*b*) Average *z*-distance between phosphorous atoms in opposite leaflets. (*c*) Average *z*-distance between cholesterol oxygens in opposite layers. All results are shown as a function of the double-bond position. Solid lines correspond to the systems with cholesterol, whereas dashed curves stand for the pure single-component bilayers (17).

substantially smaller, ~0.007 nm^2, close to the margin of error (±0.003 nm^2). Nonetheless, it is clear that A_{PC} has a maximum when the double bond resides in the middle of an acyl chain, in line with experiments (18) indicating that the main transition temperature is smallest when the double bond is located in the middle of the chain. Comparison with experimental values shows good agreement: Petrache et al. (42) obtained an average area per lipid of 0.66 nm^2 at 338 K for a DSPC bilayer (0.670 nm^2 in our simulations), and x-ray data for a fully hydrated DOPC bilayer provides a range of 0.721–0.725 nm^2 for the area per lipid (43–46) (0.731 nm^2 ± 0.003 nm^2 in our simulations).

For the PC/Chol bilayers, the area per PC is significantly smaller than for their single-component counterparts, as a signature of the condensing effect produced by cholesterol. On the other hand, the effect due to the double-bond position

TABLE 1 Average results characterizing lipid bilayer systems with 20% cholesterol

Bilayer		3	5	7	9	11	13	15	17
A_{box} (nm^2)		44.354	45.411	46.519	46.694	45.773	44.438	42.382	39.763
		46.314	**46.442**	**46.626**	**46.669**	**46.046**	**45.162**	**43.887**	**42.845**
V_{box} (nm^3)		309.43	309.84	310.15	310.07	309.94	309.79	309.53	309.33
		298.27	**298.23**	**298.36**	**298.40**	**298.49**	**298.64**	**298.83**	**299.05**
A_{PC} (nm^2)		0.629	0.644	0.660	0.663	0.649	0.630	0.602	0.564
$\pm$0.003 nm^2		**0.724**	**0.727**	**0.729**	**0.731**	**0.719**	**0.706**	**0.686**	**0.669**
P-P distance (nm)		4.13	4.12	4.05	4.04	4.11	4.22	4.39	4.64
$\pm$0.01 nm		**3.72**	**3.72**	**3.72**	**3.71**	**3.77**	**3.83**	**3.93**	**4.02**
O-O distance (nm)		0.323	0.331	0.320	0.322	0.324	0.341	0.353	0.380
$-S_{CD}$	*sn*-1	0.184	0.165	0.152	0.150	0.165	0.184	0.223	0.261
		0.106	**0.103**	**0.102**	**0.107**	**0.115**	**0.125**	**0.143**	**0.151**
	sn-2	0.192	0.168	0.153	0.152	0.164	0.185	0.219	0.262
		0.111	**0.108**	**0.105**	**0.106**	**0.116**	**0.129**	**0.144**	**0.151**
	Chol	0.188	0.170	0.154	0.156	0.168	0.183	0.212	0.288
No. of gauche	*sn*-1	2.82	3.06	3.09	3.06	2.95	2.83	2.54	2.92
		3.10	**3.21**	**3.20**	**3.17**	**3.13**	**3.08**	**2.91**	**3.50**
	sn-2	2.57	3.02	3.10	3.07	2.99	2.85	2.57	2.92
		2.90	**3.19**	**3.18**	**3.17**	**3.13**	**3.08**	**2.90**	**3.50**
Tilt angle (°)	*sn*-1	28.67	28.35	30.17	31.56	30.66	28.95	25.51	21.74
		37.57	**37.23**	**37.56**	**37.75**	**38.20**	**36.85**	**35.36**	**34.35**
	sn-2	27.55	27.62	29.44	30.65	30.44	28.29	25.48	21.06
		36.41	**36.27**	**36.78**	**36.59**	**37.46**	**35.96**	**34.74**	**33.46**
	Chol-ring	30.28	27.74	28.88	28.1	26.52	24.74	22.57	19.63
	Chol-tail	39.93	38.01	40.02	39.49	37.89	36.4	33.47	28.7
Charge pairs lipid-lipid		4.67	4.62	4.50	4.47	4.59	4.72	4.94	5.28
		4.41	**4.47**	**4.45**	**4.41**	**4.49**	**4.56**	**4.69**	**4.74**
H-bonds lipid-water		6.03	6.08	6.19	6.19	6.12	6.05	5.89	5.67
		6.40	**6.40**	**6.42**	**6.44**	**6.41**	**6.36**	**6.26**	**6.21**

Results for the single-component systems (17) are shown in bold.

is qualitatively similar to the view presented above for pure membranes. However, when cholesterol is present, the effects are much more pronounced in both directions. A clear maximum is observed in the area per PC when the double bond is placed in the middle of an acyl chain (DOPC). When the double bond approaches either the headgroup or the end of the chain, the area per PC is substantially reduced. This reduction is particularly large when the unsaturation is moved deeper into the bilayer, the largest difference being 0.099 nm^2 when DOPC is replaced with DSPC. This observation is in perfect agreement with the fact that cholesterol has a high affinity to closely interact with saturated lipids—a fact that is central to the lipid raft hypothesis (3). Comparison with experimental values shows also good agreement: DOPC bilayers with 20% of cholesterol lead to $A_{PC} = 0.673$–0.675 nm^2 (14,46), whereas we obtained 0.663 nm^2 $\pm$ 0.003 nm^2.

Membrane thickness and PC volume

To characterize the transverse structure, we calculated the thicknesses of the bilayers. We define the membrane thickness as the average distance between the phosphorous atoms in the opposite leaflets (P-P distance) (17), and plot it as a function of the double-bond position in Fig. 2 *b* (also given in Table 1). As expected, an increase in thickness is accompanied by a decrease in the average area per molecule (Fig. 2 *a*), and the thickness reaches its minimum and maximum in DOPC and DSPC, respectively. This behavior is, however, less evident when the double bond is moved from the position 9 to underneath the lipid headgroup. Fig. 2 *b* shows a comparison of membrane thicknesses in pure one-component and cholesterol-containing systems. It is evident that the addition of cholesterol amplifies the above differences. The average thickness also increases by 0.3–0.6 nm upon the addition of cholesterol. In addition, the average *z*-distance between cholesterol oxygens in opposite layers (O-O distance) is plotted in Fig. 2 *c* as a function of the double-bond position. Comparison between P-P and O-O distances reveals that the average distance between cholesterol oxygen atoms and phosphorous atoms in the same leaflet is rather uniform in all simulated bilayers, suggesting that cholesterol is equally inserted in all of the membranes. For pure DOPC, the P-P distance obtained experimentally from the phosphorous peaks in electron density profiles at 303 K varies from 3.67 to 3.71 nm (14,43–46), whereas we find a value of 3.71 $\pm$ 0.01 nm. The P-P distance can be also estimated from the length of the hydrocarbon chain, D_C, as $2[D_C + D_g]$ (14), where the length of the glycerol region, D_g, is close to 0.5 nm (43). The hydrocarbon thickness has been obtained from deuterium NMR measurements in pure DSPC bilayers at 338 K (42), resulting in 4.12 nm, whereas we find a value of 4.02 nm $\pm$ 0.01 nm.

A more detailed insight into the transverse structure of a lipid bilayer is achieved by computing the electron density profiles. The results show the typical features obtained from diffraction experiments, namely, two pronounced peaks in the phosphate group positions and a minimum in the middle of the bilayer (43). In Fig. 3 the profiles for the pure DOPC and DOPC/Chol bilayers are plotted. It is observed that when cholesterol is present, the lipid density is reduced in the region where cholesterol resides, i.e., cholesterol pushes the lipids aside from the bilayer center. This is a signature of cholesterol-induced lipid ordering that results in reducing area and increasing thickness. Moreover, inclusion of cholesterol is manifested by a reduction in system density in the middle of the bilayer that has been observed experimentally (47). The profiles in Fig. 3 show good agreement with the experimental results of Hung et al. (14). They found that addition of cholesterol up to a molar fraction of 20% in a DOPC bilayer results in a P-P distance of ~3.95 nm (see Fig. 6 in Hung et al. (14)), whereas we find 4.04 nm ± 0.01 nm in our simulations.

The average volume occupied by each PC molecule in a mixed bilayer, V_{PC}, relates the transverse and lateral structures of lipid bilayers (43), and is considered a rather conserved parameter for PC species (48), providing a good measure to compare with experimental data. In our simulations we compute V_{PC} by subtracting the volume of water and cholesterol molecules from the total simulation box volume. For the DOPC/Chol bilayer we obtain $V_{PC} = 1.335$ nm^3, whereas experimental values range from 1.296 nm^3 at 293 K to 1.303 nm^3 at 303 K (43,45). A linear extrapolation of such experimental data predicts $V_{PC} = 1.330$ nm^3 at 338K, which is very close to our result.

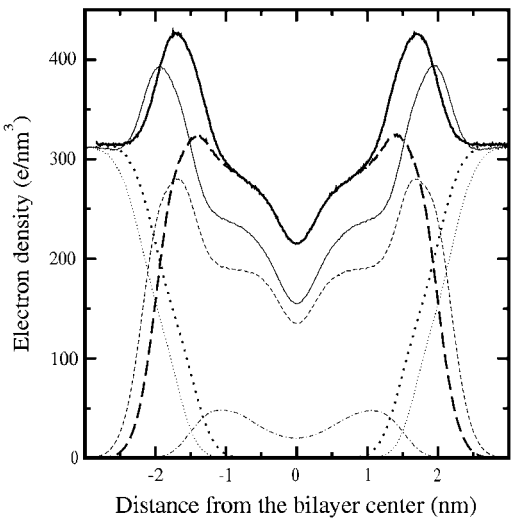

FIGURE 3 Comparison of the electron density profiles of the DOPC/Chol bilayer (*thin*) and pure DOPC bilayer (*thick*). In both cases, system (*solid*), PC (*dashed*), water (*dotted*), and cholesterol (*dot-dashed*) electron density profiles are plotted.

Order of acyl chains

To better quantify the ordering of chains, we computed the deuterium order parameter (49), S_{CD}, profiles along the chains. S_{CD} is defined as

$$S_{CD} = \left\langle \frac{3}{2}(\cos^2\theta) - \frac{1}{2} \right\rangle,$$

where θ is the angle between the CD bond and the bilayer normal, and the angular brackets denote averaging over time and over all CD bonds. Since we employed the united-atom model, the deuterium positions were constructed from the neighboring carbons assuming ideal geometries separately for single and double bonds. $-S_{CD}$ profiles along the *sn*-2 chains are plotted in Fig. 4 *a* for the PC/Chol bilayers. They show a substantial increase in chain order when the double bond is moved to the lower part of the chain. In addition, the presence of the double bond is manifested by oscillations of the S_{CD} parameter along the chain, and as a significant drop at the location of the double bond due to its conformation. Profiles for the *sn*-1 chains (not shown) are essentially similar. In Fig. 4 *b* we reproduce the $-S_{CD}$ profiles for the pure one-component bilayers (17). Our results for S_{CD} in the case of pure DSPC membranes are consistent with the experimental data (42). The dips in the order parameter profiles are due to double bonds and have been observed in a number of experimental studies (50). Comparison between Fig. 4, *a* and *b*, reveals that cholesterol strongly orders the acyl chains, particularly in their middle regions (carbon

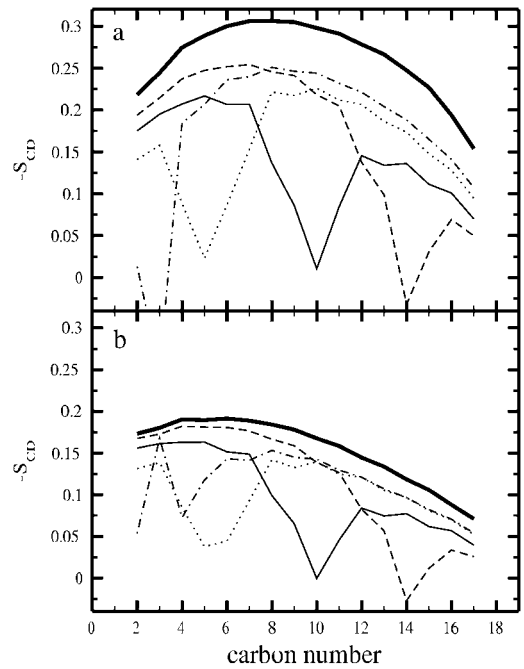

FIGURE 4 Deuterium order parameter (S_{CD}) profiles of the *sn*-2 chains for (*a*) PC/Chol bilayers and (*b*) pure PC bilayers. 18:0PC (*thick solid*), 18:1c3PC (*dot-dashed*), 18:1c5PC (*dotted*), DOPC (*solid*), and 18:1c13PC (*dashed*).

numbers 5–10) where the rigid sterol tetracyclic ring systems reside.

The mean values of S_{CD} profiles (averages over segments 4–18 with the exception of the segments containing the double bond) for the *sn*-1 and *sn*-2 PC acyl chains, and cholesterol tails, are plotted as a function of the double-bond position in Fig. 5 *a*, and the exact values are given in Table 1. For comparison, the S_{CD} averages for the one-component systems (17) are also plotted in Fig. 5 *a*. Fig. 5 *a* confirms the conclusions determined from the other quantities above: the addition of cholesterol leads to considerable ordering of the PC acyl chains and the ordering becomes strongest when the double bond is placed at the end of an acyl chain. Having the double bond in the middle of a chain has the least effect.

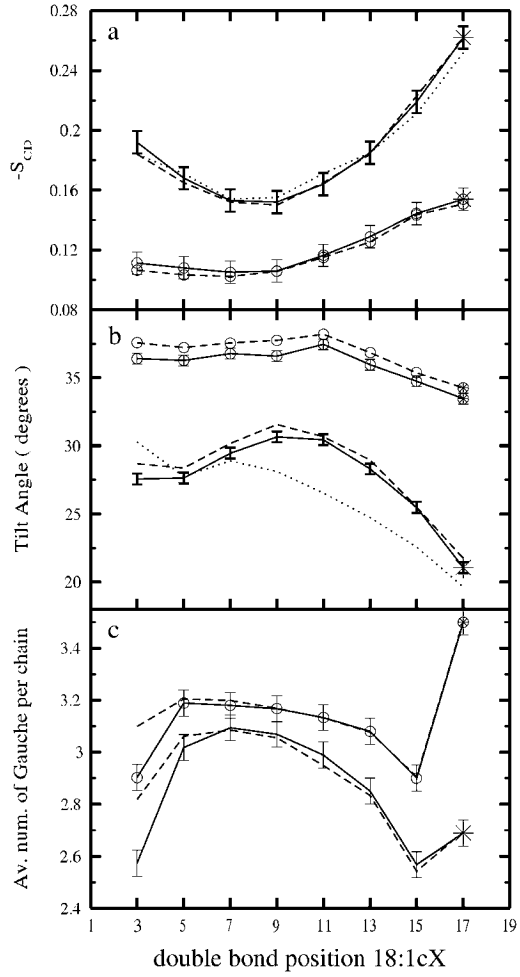

FIGURE 5 (*a*) Average values of the S_{CD} order parameter as a function of the double-bond position for both *sn*-1 (*dashed*) and *sn*-2 (*solid*) chains in the systems with and without cholesterol. The results for the tail of cholesterol are also shown (*dotted*). (*b*) Average tilt angle as a function of the position of the double bond for both *sn*-1 (*dashed*) and *sn*-2 (*solid*) chains in the systems with and without cholesterol. The tilt results for the cholesterol ring system are also provided (*dotted*). (*c*) *Gauche* number as a function of the unsaturation position for both *sn*-1 (*dashed*) and *sn*-2 (*solid*) chains in the systems with and without cholesterol. The curves with circle symbols correspond to the pure systems. Stars indicate fully saturated systems.

Orientation and conformation

The orientation of an acyl chain can be quantified by its tilt angle, defined as the angle between the bilayer normal and the vector connecting the first and last atoms in an acyl chain. In a similar manner, we defined the cholesterol ring tilt as the angle between the vector across the steroid nucleus (from C3 to C17 in Fig. 1 *b*) and the bilayer normal (9,35). Fig. 5 *b* shows the tilt averages as a function of the double bond location for the mixed bilayers. The tilts in the pure PC systems are also provided for comparison (17) (see also Table 1). In cholesterol-free membranes, the tilt remains rather constant when the double bond is placed in a position close to the interfacial membrane-water region, and only a slight increase is observed when the double bond is moved toward the middle part of the acyl chains. Moving the double bond beyond the middle part and toward the acyl tail end leads to an observable decrease of the tilt angle. For mixed bilayers, these effects are strongly amplified, and the tilt angle shows a pronounced maximum for DOPC/Chol. A more detailed consideration reveals that the cholesterol tilt remains almost constant when the double bond is close to the headgroup, whereas a significant decrease is found when the double bond crosses the middle and is moved toward the end of the acyl chains (Table 1). Finally, a comparison between Fig. 5, *a* and *b*, confirms a well established result: the smaller the sterol tilt, the stronger is the ordering ability of the sterol molecule (28,35,51).

A measure of conformational order is given by the average values of *gauche* configurations per chain (*gauche* number). A high value is indicative of a more disordered chain. Only torsion angles T4-T18 of both chains (Fig. 1 *b*) were taken into account since the third torsion angles in both *sn*-1 and *sn*-2 chains are not in well-defined and stable conformations. Angles with values 60° ± 30°, and 300° ± 30° are assigned to $gauche^+$ and $gauche^-$ conformations, respectively (36). Such averages are plotted as a function of the double-bond position in Fig. 5 *c* for both pure and mixed systems. The values for the mixed systems are provided in Table 1. The presence of cholesterol decreases the number of *gauche* conformations, a clear signature of chain ordering. In general, the qualitative behavior is similar in both systems (17). The analysis of the probability distribution of *gauche* configurations along the chain shows an increasing fraction of *gauche* bonds toward the end of the chain, as well as oscillations around the double bond (data not shown).

Surface structure and intermolecular interactions

Next, we study two possible binding modes: hydrogen (H)-bonds and charge pairs (52,53). The average number of

H-bonds between PC molecules and water characterizes lipid hydration. Such variable is plotted in Fig. 6 *a* as a function of the double-bond position for both mixed and pure systems (for the exact values see Table 1). The effect of the double-bond position follows the behavior of area per lipid: the DOPC system has the largest number of H-bonds. As in the case of the pure bilayers (17), the phosphate oxygens form the largest fraction of H-bonds with water (an average of 1.55 for each oxygen atom) since they are more exposed to the aqueous phase. The two carbonyl oxygen atoms show a rather distinct interaction with water: the one on the *sn*-2 chain (O22) forms an average of 1.47 H-bonds per oxygen, whereas the other (O32) forms only an average of 0.56 H-bonds per oxygen. This is a consequence of the fact that the *sn*-1 chains are more deeply inserted in the membrane. The presented preferential H-bonding locations are not strongly altered by the PC used in the simulation. It is important to notice, however, that the decrease in the total number of H-bonds observed for the membranes with a smaller area is mainly due to the decrease of H-bonds between water and the carbonyl oxygen atoms.

Comparison with the pure POPC bilayer simulations in Murzyn et al. (52) leads to some interesting conclusions. Despite the lower temperature of 310 K, POPC membranes display a smaller value of water H-bonds per PC (5.7) than what is found in the systems we consider. This is because lipid hydration largely depends on the area per lipid: the larger the area per lipid, the more hydrated are the lipids. In POPC simulations at 310 K, the area per molecule was 0.64 nm^2, significantly smaller than in the systems we have considered. Actually, by comparing the fraction of H-bonds with different oxygen PC atoms one realizes that H-bonding for the low temperature bilayer increases with phosphate oxygen atoms but decreases with carbonyl oxygens (compare our Table 1 with Table 1 in Murzyn et al. (52)). This may indicate that H-bonding to (outer) phosphate oxygen atoms is determined by temperature, whereas H-bonding to (inner) carbonyl oxygen atoms depends mainly on the area per lipid, i.e., on the accessibility of water molecules to such inner groups. In our simulations, the latter effect dominates. While comparing our data with those from Murzyn et al. (52), one should also take into account that both sets of results were obtained with different force fields for lipids, different water models, and different simulation setups.

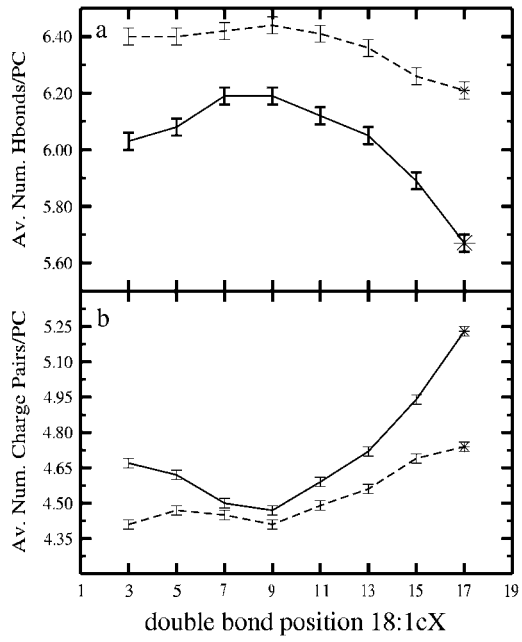

FIGURE 6 (*a*) Average number of hydrogen bonds with water per PC as a function of the double-bond position. (*b*) Average number of charge pairs involving two PC molecules (PC/PC) as a function of the unsaturation position. In both panels the solid line stands for mixed PC/Chol bilayers and the dashed line corresponds to pure PC bilayers.

The average number of H-bonds between the cholesterol hydroxyl group and the different oxygens of the PC molecules do not show any particular trend when the position of the unsaturation is varied. They do, however, display selective behavior. A clear preference of H-bonding between the hydroxyl group and the *sn*-2 carbonyl is observed (an average of 0.36 H-bonds per cholesterol molecule), as has also been found for DMPC/Chol bilayers (54). This preference results from the fact that the carbonyl in the *sn*-2 acyl chain is located closer to the surface than the carbonyl in the *sn*-1 chain, thus providing a more polar and hydrated environment to the cholesterol hydroxyl. The average number of H-bonds per cholesterol molecule is reduced to 0.08 for the *sn*-1 carbonyl. Finally, no interactions with phosphate group oxygens were observed. Such interactions would imply an exposure of the cholesterol ring nucleus to water. Finally, preferential H-bonding modes between cholesterols and PC oxygens are not substantially influenced by the location of the double bond, indicating that cholesterol is equally inserted in all of the studied systems.

Charge pairing describes the electrostatic interactions between positively (e.g., a methyl group in PC choline) and negatively (e.g., phosphate oxygens in PC or the cholesterol hydroxyl group) charged molecular moieties. In agreement with previous studies (52,53), a decrease in the surface area leads to an increase in the number of the charge pairs involving two PC molecules. This is shown in Fig. 6 *b* for both pure and mixed systems as a function of the double-bond position (Table 1).

Cholesterol ring methyl group analysis

Recent studies have shown the importance of the cholesterol off-plane C18 and C19 methyl groups in the ordering and condensing capability of cholesterol (28,55). These groups create an asymmetry in a cholesterol structure by defining its smooth (α) and rough (β) sides, and are believed to be responsible for the tilt of the sterol ring in the bilayer. Fig. 7 depicts the three-dimensional radial distribution functions (RDFs) between the centers of mass of the double bonds and

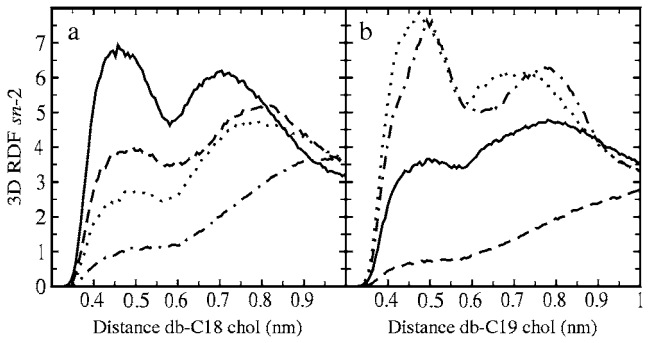

FIGURE 7 Three-dimensional RDF of the double-bond center of mass around cholesterol C18 (*a*) and C19 (*b*) methyl groups in the *sn*-2 chains. The behavior of *sn*-1 is equivalent (not shown). 18:1c3PC (*dot-dashed*), 18:1c5PC (*dotted*), DOPC (*solid*), and 18:1c13PC (*dashed*).

each one of the cholesterol methyl groups C18 and C19. The RDF curves display two clear maxima. The first peak at the distance of 0.45–0.5 nm is due to the direct interaction between the double bond and the off-plane methyl group, whereas the second at a distance of 0.7–0.8 nm corresponds to the indirect interaction across the ring (56). In our analysis we consider the first peak only, since we focus on the direct interaction.

Since the modeled interactions between the cholesterol methyl groups and the double bond are governed by van der Waals forces, Fig. 7 in part describes the strength of the attractive interaction between them, and more concretely reveals how the double bond in different monounsaturated acyl chains is distributed with respect to the C18 and C19 groups. To characterize these distributions in a more detailed manner, Fig. 8, *a* and *b* show the values of the RDFs at the approximate position of the first maximum, 0.48 nm ($I_{0.48}$), as a function of the location of the double bond. Interaction with C18 (Fig. 8 *a*) displays a maximum for DOPC. For this PC molecule, the double bond is precisely at the point where it faces the C18 group of cholesterol. Thus, the stronger the interaction between a double bond and the C18 group, the

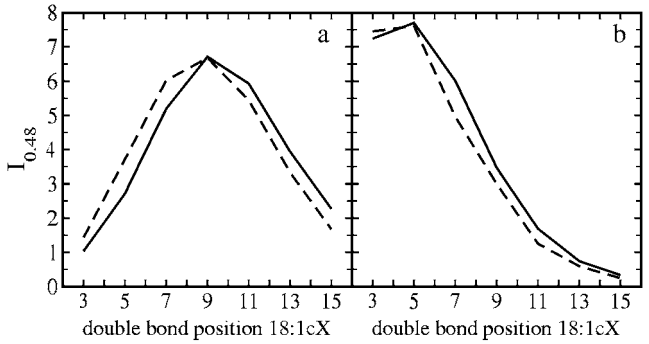

FIGURE 8 Values at 0.48 nm ($I_{0.48}$) of the three-dimensional RDFs of the double-bond center of mass around (*a*) cholesterol C18 and (*b*) C19 methyl groups for *sn*-1 (*dashed*) and *sn*-2 (*solid*) chains as a function of the double-bond position.

weaker are the ordering and condensation effects of cholesterol. This view is in agreement with the data for other unsaturated chains in Fig. 7, since if the double bond is translated away from the C18 group, packing is enhanced and the tilt of cholesterol is decreased (Table 1). Previous studies have further shown that the C18 methyl group is important in maintaining an optimal tilt of the sterol ring in a bilayer (55).

In the case of C19 (Fig. 8 *b*), the behavior is different and shows the maximum contact when the double bond is close to the water interface. In the case of DOPC, for which the condensation effect is minimized, the double bond is at the same *z*-level as the C18 group, thus impeding an optimal area condensation. When the double bond is located deeper in the membrane, the interaction with C18 is strongly reduced (double bond and C18 are placed at different *z*-levels), and the condensation effect becomes amplified. However, when the double bond is placed closer to the lipid head group, the condensation effect is amplified, mostly due to the reduction of the impediment caused by the C18 group, although the steric influence of C19 increases. The balance of these two effects determines the observed asymmetry in the general behavior: area condensation is increased when the double bond is moved toward the head group, but to a smaller extent than when moving it toward the end of the acyl chain due to the presence of C19. It seems evident that C18 is considerably more important than C19 in terms of the interplay with the double bond. This differential interaction may be explained by the fact that C18 affects a more ordered region of the acyl chains (Fig. 4 *a*) than the C19 methyl group.

DISCUSSION AND CONCLUSIONS

PCs are among the most common phospholipids in natural membranes. A major fraction of the lipid acyl chains in PCs are monounsaturated, with the double bond typically residing in the center of an acyl chain. Experimental studies have shown that the position of the double bond influences the temperature of the main phase transition T_m (32,57–61) such that lipid species with the double bond located close to the center of the chain are characterized by the lowest phase transition temperatures. Although finding a direct connection between the double bond location and the behavior of the main transition temperature is not straightforward, recent atomistic simulation studies (17) were able to shed light on this issue. It was found that membranes composed of lipids with a double bond in the middle of their chains were characterized by the largest disorder in the membrane hydrocarbon region. When the double bond was displaced from the center of an acyl chain, the disorder decreased. These findings are consistent with experiments for the dependence of T_m on the double-bond position.

Our conjecture, and the topic of this study, is that the selection of the preferred double-bond position in natural membranes is related to the interactions between PCs and cholesterol. Such an interaction can also play a crucial role in

the formation of functional platforms of ordered lipids and cholesterol, called rafts.

Comparison between the results of Martinez-Seara et al. (17) and our analysis of the atomistic MD trajectories for the PC/Chol systems clearly shows the pronounced effects of cholesterol. First, the inclusion of cholesterol in lipid bilayers leads to the well-known condensation effect. Second, as compared to the single-component bilayers, the area per PC is strongly reduced, and the membranes consistently become thicker. All these effects are accompanied by an increase in chain ordering and a reduction in the chain tilt and number of *gauche* conformations. Further, cholesterol reduces the number of H-bonds between PC molecules and water. Furthermore, our analysis shows clear nonmonotonic behavior in a number of membrane properties when the double-bond position is varied. The smallest cholesterol-induced effects were found for the DOPC/Chol bilayer. This system displayed the largest values for the membrane area and volume, acyl chain tilt, number of *gauche* conformations, and lipid hydration, and consequently the smallest membrane thickness, chain ordering, and number of charge pairs. Moving the double bond toward the lipid head group or the end of the acyl chain was observed to lead to a reduction of the area per PC. In addition, lipid chains were found to become less tilted, more ordered, and packed, and the membranes in turn became thicker, denser, and less hydrated. All of these changes are much more pronounced when the double bond is close to the end of the lipid acyl chains than when it is in the vicinity of the lipid head group. For comparison, in single-component PC bilayers the effects due to varying the double-bond position have been found to be significantly smaller or even marginal when the double bond is moved from the acyl chain center to the headgroup (17).

The nonmonotonic behavior observed for the structural membrane properties can be rationalized by looking at cholesterol/PC interactions at the atomic level. First, our results indicate that the position of cholesterol in a membrane is only weakly dependent on the location of a double bond in a lipid acyl chain, as it is mainly determined by the interaction between the sterol hydroxyl group and the *sn*-2 PC carbonyls through H-bonding. Second, the data show that the double-bond region of the PC acyl chains interacts with the C18 cholesterol methyl group most strongly when the double bond is located in the middle of an acyl chain (DOPC). As the double bond disturbs the packing of an acyl chain with the planar steroid faces, this results in a maximum in the area per molecule for the DOPC/Chol system in particular. If the double bond is translated toward the end of the chain, then its interaction with C18 is reduced, the mutual packing of Chol and PC is promoted, and the area per PC is decreased. If the double-bond position is shifted to the vicinity of the lipid head group, the interplay between the double bond and C18 is also reduced, but the influence of C19 then leads to a smaller modification of membrane properties. Our conjecture is that the interaction between C18 and the semirigid region of the PC double bond affects the tilt of cholesterol and surrounding acyl chains, and discriminates the effect of cholesterol depending on the location of the PC double bond, explaining the observed nonmonotonic behavior. The presence of C19, instead, results in the asymmetry in a number of membrane properties with respect to the middle of an acyl chain.

Let us close this work by discussing the relation of our results to a few recent experimental studies of cholesterol in unsaturated membranes (12,13). Kucerka et al. (12) varied the length of the PC chains from 14 to 22 carbons and found that the membrane thickness increased, unexpectedly, even for the longest chains. Although we did not study chains of length 22, our results provide some insight into this issue. As discussed earlier, cholesterol is equally distributed close to the membrane-water interface independently of the chain position. There is no reason to expect that this would change even for longer chains in the case of monounsaturated chains. As Figs. 2 and 5 show, cholesterol's ability to order hydrocarbon chains is remarkable and dominates over a hydrophobic mismatch. In the case of polyunsaturated chains (13), the situation may change since the introduction of several double bonds may lead to perturbations in the hydrogen bonding structure and migration of the sterol toward the center of the bilayer. Similar effects have been observed in studies of ketosterone, in which the head group is not capable of hydrogen bonding (51). This view is partly substantiated by recent coarse-grained simulations suggesting that cholesterol spends extended periods of time in the middle of a diarachidonyl-PC (DAPC; with four double bonds per acyl chain) bilayer (62).

To summarize, we have demonstrated that the presence of cholesterol clearly amplifies the nonmonotonic behavior observed in a number of structural properties of membranes with respect to the double-bond position, indicating that cholesterol contributes to the natural unsaturation heterogeneity in PC acyl chains. Even more importantly, the most obvious signs of disorder in membrane properties are found when the double bond is located close to the middle of an acyl chain, which suggests that this is a simple mechanism for promoting highly fluid membrane domains. It is obviously a means to complement rafts characterized by significant lateral as well as conformation order. It is tempting to think that the functionality of membrane domains in part arises from lipid unsaturation, and saturated and monounsaturated chains promoting the formation of raft and non-raft domains, in respective order. In these two cases the role of cholesterol is distinctly different due to its interplay with the double bond. What remains to be considered in more detail is the interplay of cholesterol with PCs with a saturated *sn*-1 and a (mono-)unsaturated *sn*-2 chain.

T. Róg holds a Marie Curie Intra-European fellowship (024612-Glychol). This work was carried out under the HPC-EUROPA project (RII3-CT-2003-506079) with the support of the European Community-Research Infrastructure Action under the FP6 ''Structuring the European Research Area'' Programme. Computational resources were provided by the Barce-

Iona Supercomputing Center (MareNostrum) and the HorseShoe cluster at the University of Southern Denmark. We thank the Academy of Finland and the Natural Sciences and Engineering Research Council of Canada (NSERC) for financial support. Partial financial support was provided by SEID through project FIS200603525, and by DURSI through project 2005-SGR000653.

REFERENCES

1. Mouritsen, O. G. 2005. Life—As a Matter of Fat. Springer, Berlin.
2. Ikonen, E. 2006. Mechanisms for cellular cholesterol transport: defects and human disease. *Physiol. Rev.* 86:1237–1261.
3. Simons, K., and E. Ikonen. 1997. Functional rafts in cell membranes. *Nature.* 387:569–572.
4. Brown, D. A., and E. London. 1998. Functions of lipid rafts in biological membranes. *Annu. Rev. Cell Dev. Biol.* 14:111–136.
5. Munro, S. 2003. Lipid rafts: elusive or illusive? *Cell* 115:377–388.
6. Niemelä, P. S., S. Ollila, M. T. Hyvönen, M. Karttunen, and I. Vattulainen. 2007. Assessing the nature of lipid raft membranes. *PLoS Comput. Biol.* 3:304–312.
7. Brown, D. A., and E. London. 2000. Structure and function of sphingolipid- and cholesterol-rich membrane rafts. *J. Biol. Chem.* 275:17221–17224.
8. Simons, K., and D. Toomre. 2000. Lipid rafts and signal transduction. *Mol. Cell. Biol.* 1:31–41.
9. Vainio, S., M. Jansen, M. Koivusalo, T. Róg, I. Vattulainen, and E. Ikonen. 2006. Demosterol cannot replace cholesterol in lipid rafts. *J. Biol. Chem.* 281:348–355.
10. Soubias, O., and K. Gawrisch. 2005. Probing specific lipid-protein interaction saturation transfer difference NMR spectroscopy. *J. Am. Chem. Soc.* 127:13110–13111.
11. Qin, L., M. A. Sharpe, R. M. Garavito, and S. Ferguson-Miller. 2007. Conserved lipid-binding sites in membrane proteins: a focus on cytochrome *c* oxidase. *Curr. Opin. Struct. Biol.* 17:444–450.
12. Kucerka, N., J. Pencer, M.-P. Nieh, and J. Katsaras. 2007. Influence of cholesterol on the bilayer properties of monounsaturated phosphatidylcholine unilamellar vesicles. *Eur. Phys. J. E.* 23:247–254.
13. Harroun, T. A., J. Katsaras, and S. R. Wassall. 2006. Cholesterol hydroxyl group found to reside in the center of a polyunsaturated lipid membrane. *Biochemistry.* 45:1227–1233.
14. Hung, W.-C., M.-T. Lee, F.-Y. Chen, and H. W. Huang. 2007. The condensing effect of cholesterol in lipid bilayers. *Biophys. J.* 92:3960–3967.
15. Gallova, J., D. Uhrikova, M. Hanulova, J. Texeira, and P. Balgavy. 2004. Bilayer thickness in unilamellar extruded 1,2-dimyristoleoyl and 1,2-dierucoyl phosphatidilcholine vesicles: SANS contrast variation study of cholesterol effect. *Colloids Surf. B Biointerfaces.* 38:11–14.
16. Olsson, N. U., and N. Salem Jr. 1997. Molecular species analysis of phospholipids. *J. Chromatogr. B Analyt. Technol. Biomed. Life Sci.* 692:245–256.
17. Martinez-Seara, H., T. Róg, M. Pasenkiewicz-Gierula, I. Vattulainen, M. Karttunen, and R. Reigada. 2007. Effect of double bond position on lipid bilayer properties: insight through atomistic simulations. *J. Phys. Chem. B.* 111:11162–11168.
18. Marsh, D. 1999. Thermodynamic analysis of chain-melting transition temperatures for monounsaturated phospholipid membranes: dependence on cis-monoenoic double bond position. *Biophys. J.* 77:953–963.
19. Ollila, S., T. Róg, M. Karttunen, and I. Vattulainen. 2007. Role of sterol type on lateral profiles of lipid membranes affecting membrane protein functionality: comparison between cholesterol, desmosterol, 7-dehydrocholesterol and ketosterol. *J. Struct. Biol.* 159:311–323.
20. Lindahl, E., B. Hess, and D. van der Spoel. 2001. GROMACS 3.0: a package for molecular simulation and trajectory analysis. *J. Mol. Model.* 7:306–317.
21. Van der Spoel, D., E. Lindahl, B. Hess, G. Groenhof, A. E. Mark, and H. J. C. Berendsen. 2005. GROMACS: fast, flexible, and free. *J. Comput. Chem.* 26:1701–1718.
22. Berger, O., O. Edholm, and F. Jahnig. 1997. Molecular dynamics simulations of a fluid bilayer of dipalmitoylphosphatidylcholine at full hydration, constant pressure, and constant temperature. *Biophys. J.* 72:2002–2013.
23. Patra, M., M. Karttunen, M. T. Hyvönen, E. Falck, and I. Vattulainen. 2004. Lipid bilayers driven to a wrong lane in molecular dynamics simulations by truncation of long-range electrostatic interactions. *J. Phys. Chem. B.* 108:4485–4494.
24. Tieleman, D. P., and H. J. C. Berendsen. 1996. Molecular dynamics simulations of a fully hydrated dipalmitoylphosphatidylcholine bilayer with different macroscopic boundary conditions and parameters. *J. Chem. Phys.* 105:4871–4880.
25. Bachar, M., P. Brunelle, D. P. Tieleman, and A. Rauk. 2004. Molecular dynamics simulation of a polyunsaturated lipid bilayer susceptible to lipid peroxidation. *J. Phys. Chem. B.* 108:7170–7179.
26. Berendsen, H. J. C., J. P. M. Postma, W. F. van Gunsteren, and J. Hermans. 1981. Interaction models for water in relation to protein hydration. *In* Intermolecular Forces. B. Pullman, editor. Reidel, Dordrecht, The Netherlands.
27. Holtje, M., T. Forster, B. Brandt, T. Engels, W. von Rybinski, and H.-D. Holtje. 2001. Molecular dynamics simulations of stratum corneum lipid models: fatty acids and cholesterol. *Biochim. Biophys. Acta.* 1511:156–167.
28. Róg, T., I. Vattulainen, M. Pasenkiewicz-Gierula, and M. Karttunen. 2007. What happens if cholesterol is made smoother: importance of methyl substituents in cholesterol ring structure on phosphatidylcholine-sterol interactions. *Biophys. J.* 92:3346–3357.
29. Miyamoto, S., and P. A. Kollman. 1992. SETTLE: an analytical version of the SHAKE and RATTLE algorithms for rigid water models. *J. Comput. Chem.* 13:952–962.
30. Hess, B., H. Bekker, H. J. C. Berendsen, and J. G. E. M. Fraaije. 1997. LINCS: a linear constraint solver for molecular simulations. *J. Comput. Chem.* 18:1463–1472.
31. Essman, U., L. Perera, M. L. Berkowitz, H. L. T. Darden, and L. G. Pedersen. 1995. A smooth particle mesh Ewald method. *J. Chem. Phys.* 103:8577–8592.
32. Koyanova, R., and M. Caffrey. 1998. Phases and phase transitions of the phosphatidylcholines. *Biochim. Biophys. Acta.* 1376:91–145.
33. Berendsen, H. J. C., J. P. M. Postma, W. F. van Gunsteren, A. DiNola, and J. R. Haak. 1984. Molecular dynamics with coupling to an external bath. *J. Chem. Phys.* 81:3684–3690.
34. Niemelä, P. S., M. T. Hyvönen, and I. Vattulainen. 2006. Influence of chain length and unsaturation on sphingomyelin bilayers. *Biophys. J.* 90:851–863.
35. Aittoniemi, J., T. Róg, P. Niemelä, M. Pasenkiewicz-Gierula, M. Karttunen, and I. Vattulainen. 2006. Tilt: major factor in sterols' ordering capability in membranes. *J. Phys. Chem. B.* 110:25562–25564.
36. Róg, T., and M. Pasenkiewicz-Gierula. 2001. Cholesterol effects on the phosphatidylcholine bilayer nonpolar region: a molecular simulation study. *Biophys. J.* 81:2190–2202.
37. Falck, E., M. Patra, M. Karttunen, M. T. Hyvönen, and I. Vattulainen. 2004. Lessons of slicing membranes: interplay of packing, free area, and lateral diffusion in phospholipid/cholesterol bilayers. *Biophys. J.* 87:1076–1091.
38. Hess, B. 2002. Determining the shear viscosity of model liquids from molecular dynamics simulations. *J. Chem. Phys.* 116:209–217.
39. Edholm, O., and J. F. Nagle. 2005. Areas of molecules in membranes consisting of mixtures. *Biophys. J.* 89:1827–1832.
40. Hofsäß, C., E. Lindahl, and O. Edholm. 2003. Molecular dynamics simulations of phospholipid bilayers with cholesterol. *Biophys. J.* 84: 2192–2206.

41. Chiu, S. W., E. Jacobsson, R. J. Mashl, and H. L. Scott. 2002. Cholesterol-induced modifications in lipid bilayers: a simulation study. *Biophys. J.* 83:1842–1853.

42. Petrache, H. I., S. W. Dodd, and M. F. Brown. 2000. Area per lipid and acyl chain length distributions in fluid phosphatidylcholines determined by ^{2}H-NMR spectroscopy. *Biophys. J.* 79:3172–3192.

43. Nagle, J. F., and S. Tristram-Nagle. 2000. Structure of lipid bilayers. *Biochim. Biophys. Acta.* 1469:159–195.

44. Liu, Y., and J. F. Nagle. 2004. Diffuse scattering provides material parameters and electron density profiles of biomembranes. *Phys. Rev. E Stat. Nonlin. Soft Matter Phys.* 69:040901 (R).

45. Kucerka, N., S. Tristram-Nagle, and J. F. Nagle. 2005. Structure of fully hydrated fluid phase lipid bilayers with monounsaturated chains. *J. Membr. Biol.* 208:193–202.

46. Mathai, J. C., S. Tristram-Nagle, J. F. Nagle, and M. L. Zeidel. 2008. Structural determinants of water permeability through the lipid membrane. *J. Gen. Physiol.* 131:69–76.

47. Subczynski, W. K., A. Wisniewska, J.-J. Yin, J. S. Hyde, and A. Kusumi. 1994. Hydrophobic barriers of lipid bilayer membranes formed by reduction of water penetration by alkyl chain unsaturation and cholesterol. *Biochemistry.* 33:7670–7681.

48. Pan, D., W. Wangchen, W. Liu, L. Yang, and H. W. Huang. 2006. Chain packing in the inverted hexagonal phase of phospholipids: a study by x-ray anomalous diffraction on bromine-labeled chains. *J. Am. Chem. Soc.* 128:3800–3807.

49. Davis, J. H. 1983. The description of membrane lipid conformation, order and dynamics by ^{2}H-NMR. *Biochim. Biophys. Acta.* 737:117–171.

50. Ollila, S., M. T. Hyvonen, and I. Vattulainen. 2007. Polyunsaturation in lipid membranes: dynamic properties and lateral pressure profiles. *J. Phys. Chem. B.* 111:3139–3150.

51. Rog, T., L. M. Stimson, M. Pasenkiewicz-Gierula, I. Vattulainen, and M. Karttunen. 2008. Replacing the cholesterol hydroxyl group by the ketone group facilitates sterol flip-flop and promotes membrane fluidity. *J. Phys. Chem. B.* 112:1946–1952.

52. Murzyn, K., T. Róg, G. Jezierski, K. Kitamura, and M. Pasenkiewicz-Gierula. 2001. Effects of phospholipid unsaturation on the membrane/water interface: a molecular simulation study. *Biophys. J.* 81:170–183.

53. Murzyn, K., W. Zhao, M. Karttunen, M. Kurdziel, and T. Róg. 2006. Dynamics of water at membrane surfaces effect of headgroup structure. *Biointerphases.* 1:98–105.

54. Czub, J., and M. Baginski. 2006. Comparative molecular dynamics study of lipid membranes containing cholesterol and ergosterol. *Biophys. J.* 90:2368–2382.

55. Pöyry, S., T. Róg, M. Karttunen, and I. Vattulainen. 2008. Significance of cholesterol methyl groups. *J. Phys. Chem. B.* 112:2922–2929.

56. Róg, T., and M. Pasenkiewicz-Gierula. 2004. Non-polar interactions between cholesterol and phospholipids: a molecular dynamics study simulation. *Biophys. Chem.* 107:151–164.

57. Seelig, A., and J. Seelig. 1977. Effect of a single *cis* bond on the structure of a phospholipids bilayer. *Biochemistry.* 16:45–50.

58. Stubbs, C., and A. D. Smith. 1984. The modification of mammalian membrane polyunsaturated fatty acid composition in relation to membrane fluidity and function. *Biochim. Biophys. Acta.* 779:89–137.

59. Huang, C. H. 2001. Mixed-chain phospholipids: structures and chain melting behavior. *Lipids.* 36:1077–1097.

60. Wang, G., H. N. Lin, S. Li, and C. H. Huang. 1995. Phosphatidylcholine with *sn-1* saturated and *sn-2 cis*-monounsaturated acyl chains. *J. Biol. Chem.* 270:22738–22746.

61. Seelig, J., and N. Waespe-Šarčević. 1978. Molecular order in *cis* and *trans* unsaturated phospholipid bilayers. *Biochemistry.* 17:3310–3315.

62. Marrink, S. J., A. H. de Vries, T. A. Harroun, J. Katsaras, and S. R. Wassall. 2008. Cholesterol shows preference for the interior of polyunsaturated lipid membranes. *J. Am. Chem. Soc.* 130:10–11.